Supercritical Fluid and Compressed Solvent Effects on Metallic Nanoparticle Synthesis in Reverse Micelles

Joanna P. Cason, Kedar Khambaswadkar, and Christopher B. Roberts*

Department of Chemical Engineering, 230 Ross Hall, Auburn University, Alabama 36849

This paper presents the formation of nanosized metallic particles synthesized in sodium bis(2-ethylhexyl)sulfosuccinate (AOT) reverse micelles in compressed propane and supercritical fluid (SCF) ethane solutions. Silver nanoparticles were produced in AOT reverse micelles in compressed propane by the reduction of the silver salt, $AgNO_3$. Copper nanoparticles were produced in compressed propane and SCF ethane solvents, with added isooctane cosolvent, by the reduction of the functionalized surfactant, $Cu(AOT)_2$. Particle growth rates in the compressed fluids are compared with those in normal liquid solvents to illustrate the effects of the compressed fluids on the growth behavior of these nanoparticles within the reverse micelles. The metallic nanoparticles were characterized using both in situ UV−vis spectroscopy and transmission electron microscopy. The use of compressed fluids and SCFs for nanoparticle formation in AOT reverse micelles can result in growth rate behavior different from that in normal liquid solvents for both copper and silver. This is the result of the intermediate physical and transport properties of the compressed and supercritical solvents which lead to enhanced collision frequencies and exchange rates between micelles.

Introduction

There is a great deal of interest in the preparation and applications of nanometer-sized materials.[1] Reverse micelles in normal liquid solvents have been widely employed as "nanoreactors" within which to carry out controlled reactions, leading to the formation of colloidal metallic particles and semiconductor crystallites.[2] Reverse micelles are thermodynamically stable aggregates of amphiphilic surfactants, resulting in a hydrophilic headgroup region surrounding a nanosized water core with hydrophobic tails that extend into a nonpolar continuous phase. A variety of polar and ionic species can be dissolved within the water cores, which are dispersed in the continuous phase solvent. The size of the micelle core is characterized by the molar ratio of water to surfactant molecules in the solution, W (=$[H_2O]$/[surfactant]). Among the more common surfactants used for the formation of reverse micelles in organic solvents is the anionic surfactant sodium bis(2-ethylhexyl)-sulfosuccinate (commonly known as AOT).

There have been numerous studies which have reported the synthesis of nanometer-sized organic and inorganic materials within the water cores of these normal liquid reverse micelles. Several review papers have been published which contain work on the production of silver, copper, and other metal nanoparticles, as well as various semiconductor crystallites.[2−4] The production of metallic copper and silver particles has been studied in detail by simple reduction reactions within the cores of AOT reverse micelles in normal liquid hydrocarbon solvents.[5−9] These papers describe that the size of the metallic particles after a fixed reaction time was influenced primarily by the water content of the micelle, W, the average number of metal ions and reducing agent molecules per micelle, and the continuous phase solvent type.

Reverse micelles in solution will exchange the contents of their cores via both fusion and redispersion processes.[10] Therefore, the reduction of a metal salt within the cores of reverse micelles can result in the growth of nanometer-sized metal particles. This occurs because of random collisions of the micelles, which cause an exchange of the reactants between micelles. This collision results in fusion of the micelles, diffusion of the contents within the cores, and redispersion of the micelles.[10,11] Depending on the rate of the chemical reaction, particle production can be controlled by this intermicellar exchange rate.[12,13] This intermicellar exchange rate can be influenced by several factors that affect the attractive interactions between micelles including the size of the micelle core, the properties of the bulk solvent, and the strength of the interactions between the solvent and the surfactant tails.[7,11] Bagwe and Khilar[11] found that the solvent properties can play an important role in the dynamics of nanoparticle formation through their influence on the attractive interactions between micelles. Given that this particle synthesis process can be affected by changes in the continuous phase solvent, the use of compressed gases and supercritical fluid (SCF) solvents can provide further influence through their adjustable physicochemical solvent properties.[14]

Studies of AOT microemulsions in SCFs and compressed solvents have only appeared in the literature since the discovery of AOT reverse micelles in SCFs by Gale et al. in 1987.[15] Since that time, many studies have been performed to examine the structure of AOT reverse micelles in compressible fluids. Recently, Bartscherer et al.[16] reviewed many of these works, and, in general, they have shown the ability to produce thermodynamically stable AOT reverse micelles for which there is essentially no change in the size and interior polarity with changes in the pressure in a single-phase system. However, attractive intermicellar interactions may become enhanced at low pressures.

* To whom correspondence should be addressed. E-mail: croberts@eng.auburn.edu. Fax: (334) 844-2063.

10.1021/ie000147z CCC: $19.00
Published on Web 11/15/2000

Recently, a few inorganic reactions in reverse micelles in SCFs have been reported. Matson et al.[17] reported the production of $Al(OH)_3$ particles in AOT reverse micelles in supercritical propane. Clarke et al.[18] demonstrated reactions of $Na_2[Fe(CN_5)(NO)]$ and K_2CrO_7 with gaseous reactants in SCF CO_2 microemulsions stabilized by perfluoropolyether (PFPE) surfactant. More recently, Ji et al.[19] described the synthesis and dispersion of silver nanoparticles in a water-in-CO_2 microemulsion. In addition, Holmes and co-workers[20] have recently presented the synthesis of cadmium sulfide particles in water-in-CO_2 microemulsions.

Here we present the formation of nanosized silver particles within AOT reverse micelles in a compressed propane solvent. We also demonstrate the production of nanometer-sized metallic copper particles by chemical reaction in AOT reverse micelles in compressed propane and SCF ethane solutions.

Experimental Section

Materials. The surfactant AOT was purchased from Fisher Scientific. Hydrazine (98%, anhydrous; N_2H_4), sodium borohydride ($NaBH_4$), and silver nitrate ($AgNO_3$) were purchased from Aldrich. Propane and ethane were purchased from BOC Gases. Isooctane and cyclohexane (99+%) were purchased from Acros. All were used without further purification. Copper AOT [$Cu(AOT)_2$], produced in our lab by a method previously described in the literature,[5] was used as the copper ion source in the reduction reactions.

Experimental Procedure. The reactions were performed in a fixed-volume stainless steel reactor fitted with two quartz windows to allow UV−vis measurements to be made. The solid reactants were loaded into the vessel, which was then sealed and purged with nitrogen prior to the addition of water and liquid cosolvent (when necessary). The bulk solvent was then injected into the vessel using an ISCO 260D high-pressure syringe pump until the desired pressure was attained. After the contents were allowed to mix for several hours and thermal equilibrium was reached, the reaction was initiated by the addition of a reducing agent through a B-100-S Eldex metering pump or an external injection loop and then mixing was ceased (no agitation during the reaction). The pressure inside the vessel was monitored to ±0.2 bar using a 901A Heise pressure gauge, and a heating tape, platinum RTD, and an Omega 6071A controller were used to maintain the cell temperature to within ±0.1 °C. UV−vis spectra were acquired at fixed time intervals throughout the reaction on a Varian 3E UV−vis spectrophotometer.

Metallic silver nanoparticles were produced in compressed liquid propane at 37 °C, 200 bar, and a W of 10 with AOT, $AgNO_3$, and $NaBH_4$ concentrations of 1×10^{-1}, 1×10^{-3}, and 3×10^{-3} M, respectively. Copper nanoparticles were also produced by reduction of $Cu(AOT)_2$ with a N_2H_4 reducing agent in compressed liquid propane solvent, with a 7% (v/v) isooctane cosolvent, at a pressure of 145 bar, and at a temperature of 30 °C. The reagent concentrations used were 7×10^{-2} M NaAOT and 7×10^{-3} M $Cu(AOT)_2$ with a W value of 10. Copper nanoparticles were also synthesized in a SCF ethane solvent with a 14% (v/v) isooctane cosolvent at 255 bar at 37 °C with reagent concentrations of 5×10^{-2} M NaAOT and 5×10^{-3} M $Cu(AOT)_2$ at a W of 7.8.

Samples for transmission electron microscope (TEM) analysis were either prepared by transferring a small droplet of liquid solution with dispersed particles onto a carbon type-A 400 mesh nickel grid or by directly spraying the reactor contents onto a TEM grid and evaporating under vacuum. Electron micrographs were obtained on a Zeiss EM 10 TEM.

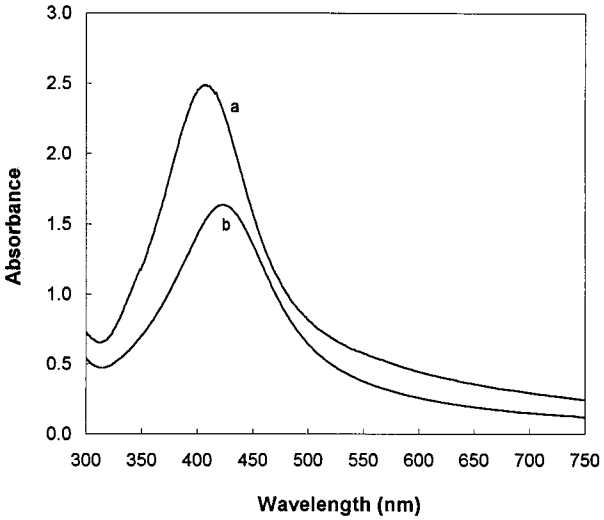

Figure 1. UV−vis absorption spectra of silver nanoparticles in AOT reverse micelles (a) in compressed propane and (b) resuspended in ethanol. $W_o = 10$, $T = 37$ °C, $P = 200$ bar, [AOT] = 1×10^{-1} M, [$AgNO_3$] = 1×10^{-3} M, and [$NaBH_4$] = 3×10^{-3} M.

Collection Methods. Many of the applications of these nanomaterials would require their removal from the high-pressure reactor and their deposition onto a surface. While many methods could be developed, we describe three methods that we have employed for the recovery of these nanoparticles from a high-pressure solution. (1) One method involves the transfer of the reactor contents into a liquid micellar solution. A portion of the contents of the high-pressure reactor was bubbled into a liquid isooctane/AOT solution with the same W and AOT concentration. The recovered solution was then quickly analyzed using both UV−vis spectroscopy and TEM. In this way, the reaction largely took place in the high-pressure reactor with minimal residence in the liquid solvent. (2) The nanoparticles were also recovered by slowly depressurizing the high-pressure vessel, allowing the surfactant mixture containing the nanoparticles to collapse on the bottom of the vessel, as described by Holmes et al.[20] This surfactant matrix was collected and dissolved in ethanol, allowing the particles to be redispersed into solution. This solution was then analyzed using both UV−vis spectroscopy and TEM. (3) The final collection method employed here involves the rapid expansion of the reactor contents directly onto a TEM grid, as described by Ji et al.[19] While this method does not allow UV−vis spectra to be obtained, it does provide a direct means of application of the particles onto a surface.

Results and Discussion

Nanoparticle Synthesis. The first series of experiments presented here demonstrate the production of silver nanoparticles by the reduction of a silver salt, $AgNO_3$, dissolved within the water core of AOT reverse micelles by a sodium borohydride reducing agent, $NaBH_4$. Silver particle formation was initially performed within the AOT reverse micelles with compressed propane as the bulk solvent. Figure 1 shows an

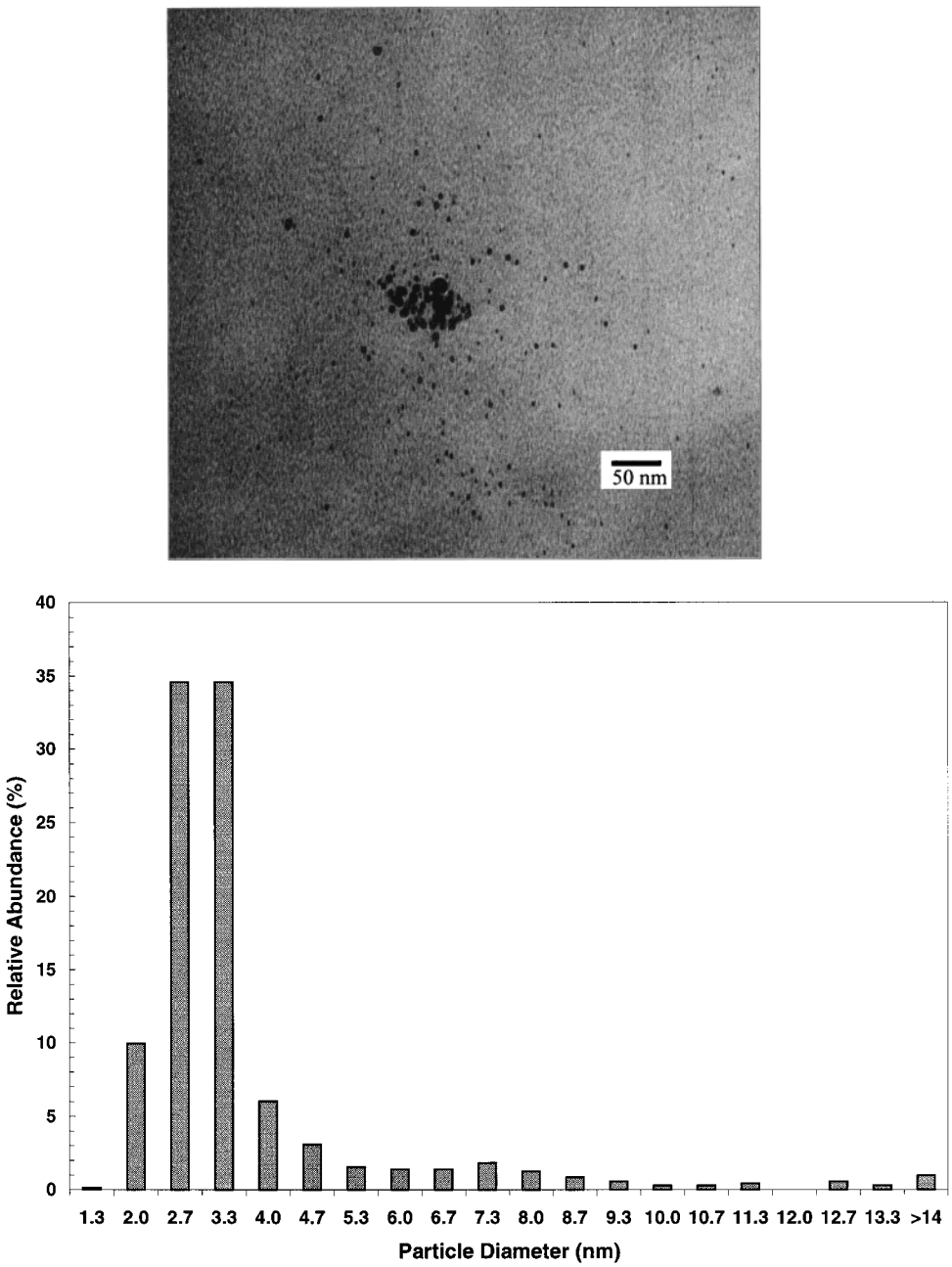

Figure 2. (A) Example of TEM and (B) particle size distribution of silver particles recovered from compressed propane and collected via redispersion in ethanol. $W_o = 10$, $T = 37$ °C, $P = 200$ bar, [AOT] $= 1 \times 10^{-1}$ M, [$AgNO_3$] $= 1 \times 10^{-3}$ M, and [$NaBH_4$] $= 3 \times 10^{-3}$ M. More than 780 particles were sized from six micrographs for the size distribution (see text).

example of the characteristic absorption spectra for metallic silver nanoparticles produced in compressed liquid propane at 37 °C, 200 bar, and a W of 10. The AOT, $AgNO_3$, and $NaBH_4$ concentrations used were 1×10^{-1}, 1×10^{-3}, and 3×10^{-3} M, respectively. Fortunately, colloidal dispersions of silver absorb in the UV−vis range, allowing in situ measurements to be made. The characteristic absorption spectrum for silver nanoparticles has a peak at approximately 400 nm, and as the particle size is increased, the absorption spectrum becomes narrower with an increase in the intensity of the band and a decrease in the bandwidth.[8,9] Furthermore, there is a linear variation of the half-width with the inverse of the particle diameter.[21] Petit and coworkers[9] present such a linear relationship for silver particles produced in AOT reverse micelles where the size of the silver nanoparticles can be estimated from absorption spectra using the following correlation based on the full width at half-maximum (FWHM) of the peak:[9]

$$\mathrm{FWHM} = 50 + 2300/D \qquad (1)$$

where FWHM is in nanometers and D, the particle diameter, is in angstroms. If eq 1 is applied here, the particle size was found to range from approximately 3.5 to 4.7 nm over a period of 15 min. Figure 2A shows an example of a TEM micrograph containing nanosized silver particles produced in a compressed propane solvent. The silver nanoparticles were recovered by slowly depressurizing the high-pressure vessel, allowing the surfactant containing the nanoparticles to collapse on the bottom of the vessel, as described by Holmes et al.[20] This nanoparticle/surfactant matrix was collected,

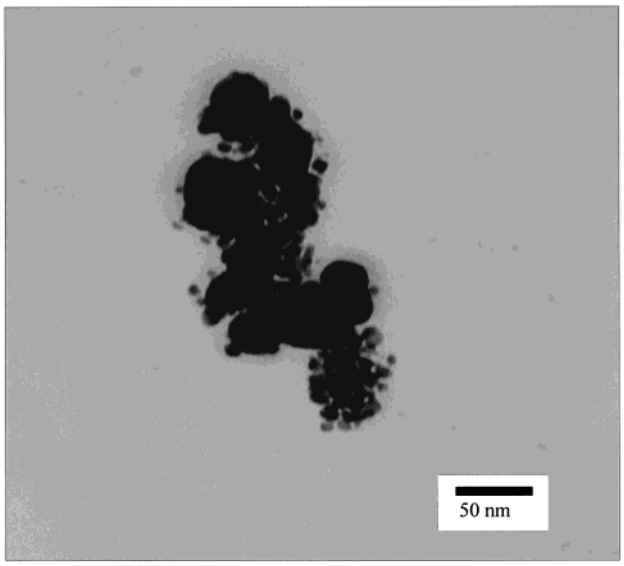

Figure 3. TEM of silver particles produced in compressed propane and recovered by rapid expansion method. $W_o = 10$, $T = 37$ °C, $P = 200$ bar, [AOT] $= 1 \times 10^{-1}$ M, [$AgNO_3$] $= 1 \times 10^{-3}$ M, and [$NaBH_4$] $= 3 \times 10^{-3}$ M.

and the particles were redispersed in ethanol. This ethanol solution was analyzed on the UV−vis spectrometer, and the spectrum is shown in Figure 1 (line b). A droplet of this solution was then placed on a TEM grid and analyzed directly. Figure 2B presents a histogram of the particle size distribution obtained by measuring the diameter of all of the particles (more than 780 particles) from six micrographs from different parts of the grid (×150 000). The mean particle size and standard deviation are 3.8 and 2.4 nm, respectively, with more than 88% of the particles being less than 5 nm and less than 1% of the particles being greater than 14 nm. The mean particle size of 3.8 nm is comparable to the particle size range of 3.5−4.7 nm suggested by the analysis of the absorption spectra using eq 1.

The silver nanoparticles produced in compressed liquid propane at 37 °C, 200 bar, and a W of 10 were also collected by rapid expansion of the reactor contents directly onto a TEM grid, as described by Ji et al.[19] This technique provides a direct means of application of the particles onto a surface. As seen in Figure 3, the silver nanoparticles collected in this way are clustered and slightly larger in size than those obtained from the redispersion method above.

The next series of experiments described here demonstrate the formation of copper nanoparticles in a compressed liquid propane solvent at a pressure of 145 bar and a temperature of 30 °C. The reagent concentrations were 7×10^{-2} M NaAOT and 7×10^{-3} M $Cu(AOT)_2$ with a W value of 10. A small amount of isooctane [7% (v/v)] was added as a cosolvent to increase the bulk solvent density and to promote complete solubility of the surfactants as determined from visual observation of the phase behavior using the optical windows in the reactor. Figure 4 (line a) presents the characteristic absorption spectrum of nanosized copper particles produced in compressed propane with isooctane cosolvent only 15 min after hydrazine injection. This absorption occurs because of the excitation of plasma resonances or interband transitions and is centered at 566 nm for copper.[6,22] Yanase and Komiyama[23] have shown that the formation of copper oxide is evidenced by the appearance of a residual absorption

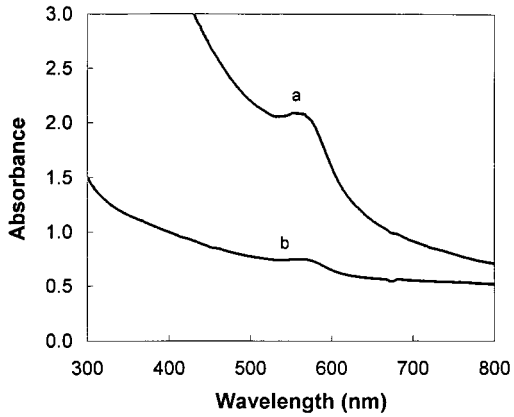

Figure 4. Characteristic UV−vis absorption spectra of nanosized copper particles produced in compressed propane both (a) in situ and (b) resuspended in liquid isooctane. [AOT] $= 7 \times 10^{-2}$ M, [$Cu(AOT)_2$] $= 7 \times 10^{-3}$ M, $W = 10$, $P = 145$ bar, and $T = 30$ °C.

at 800 nm. In these studies, the reaction vessel was heavily purged with nitrogen prior to reduction and an appearance of a residual absorbance at 800 nm due to copper oxide was not observed. Lisiecki and Pileni[7] have demonstrated that a ratio of the absorbance at the maximum of the characteristic plasmon peak which occurs at 566 nm to the absorbance off of the peak at 500 nm ($\epsilon_{566}/\epsilon_{500}$) can be used to calibrate the particle size. In short, this ratio increases with increasing particle size. According to the reported calibration curve of Lisiecki and Pileni,[7] the ratio of $\epsilon_{566}/\epsilon_{500}$ from the in situ absorption spectra shown in Figure 4 (line a) corresponds to a particle size of approximately 9 nm. Unfortunately, absorption measurements could not be made after this initial 15 min period because of the high absorption produced in the large path length (7 cm) of the reactor. After the reaction had proceeded to a point where absorption measurements could no longer be made, a portion of the contents of the high-pressure reactor was bubbled into a liquid isooctane/AOT solution with the same W and AOT concentration. This recovered solution was quickly analyzed on UV−vis, and a TEM grid was prepared. In this way, the reaction largely took place in the compressed propane with minimal residence in the liquid solvent. The UV−vis absorption spectrum of the copper nanoparticles in this liquid isooctane solution is shown in Figure 4 (line b). While the overall absorbance is significantly lower because of dilution during collection, the characteristic copper peak centered at 566 nm is still apparent. The ratio of $\epsilon_{566}/\epsilon_{500}$ from this recovered sample corresponds to a particle size of approximately 10 nm according to the calibration curve of Lisiecki and Pileni,[7] although there is greater uncertainty in this measurement because of the low overall absorbance. This varies only 1 nm from the 9 nm particle size indicated in the in situ absorption spectrum, suggesting that the collection procedure may have had little influence on the nanoparticle products and demonstrating that this as a viable collection alternative from high-pressure dispersions. Figure 5 presents examples of TEM micrographs of copper nanoparticles as produced in the compressed propane mixture and recovered through this transfer method. The average size of the particles as measured from the TEM micrographs is approximately 18 nm ± 5 nm. The larger size compared to that indicated by the in situ UV−vis spectra could be attributed to a small degree of particle agglomeration that may occur during the collection

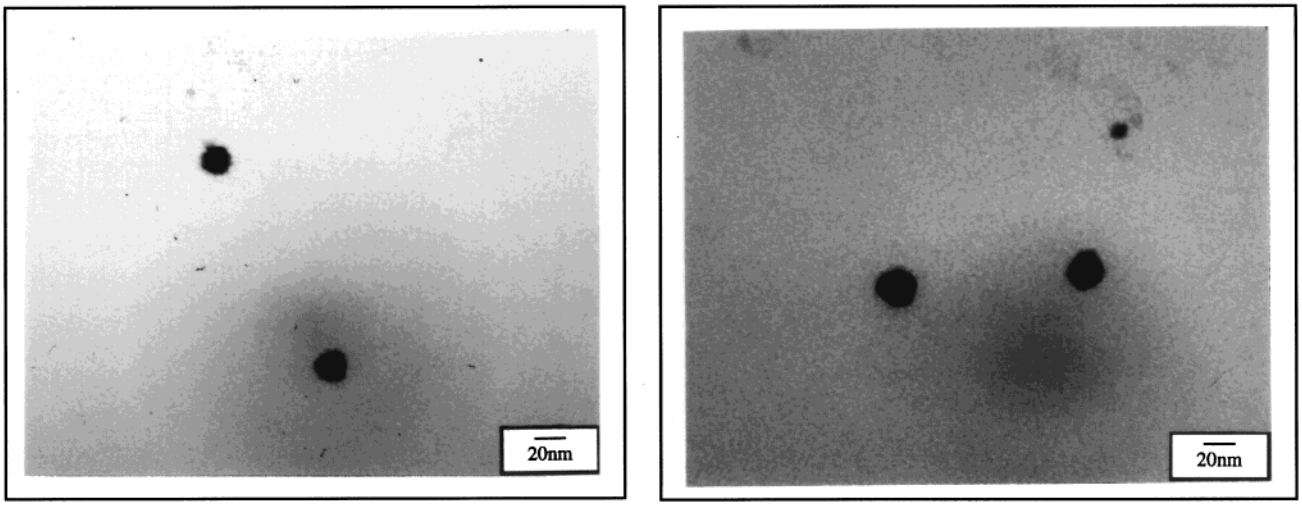

Figure 5. Examples of TEM of nanosized metallic copper particles produced in compressed propane. [AOT] = 7×10^{-2} M, [$Cu(AOT)_2$] = 7×10^{-3} M, $W = 10$, $P = 145$ bar, and $T = 30$ °C.

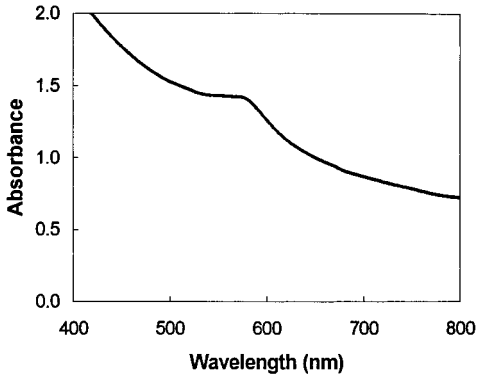

Figure 6. Characteristic UV−vis absorption spectrum of nanosized copper particles produced in SCF ethane at a reaction time of 1 h. The conditions of the ethane experiment were [NaAOT] = 5×10^{-2} M, [$Cu(AOT)_2$] = 5×10^{-3}, $W = 7.8$, 14% (v/v) isooctane, $P = 245$ bar, and $T = 37$ °C.

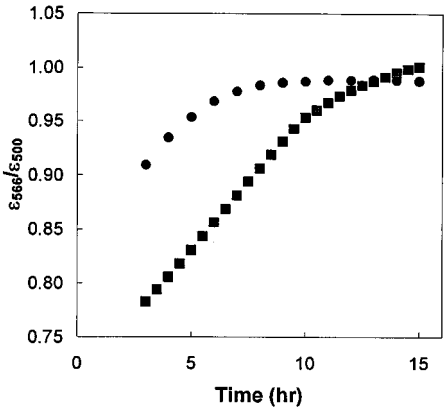

Figure 7. Comparison of growth curves for copper nanoparticles in liquid isooctane (●) and liquid cyclohexane (■). [AOT] = 1×10^{-1} M, [$Cu(AOT)_2$] = 1×10^{-2} M, [N_2H_4] = 3×10^{-2} M, and $W = 5$.

procedure, to the fact that the particles were collected some time after the absorption measurement was made, or possibly to some degree of error associated with applying the calibration curve ($\epsilon_{566}/\epsilon_{500}$) of Lisiecki and Pileni[7] which was constructed for normal liquids.

The copper nanoparticle synthesis was also was performed in a SCF ethane solvent mixture. Because of the low solvent strength of ethane compared to propane,[15,16] a pressure of 255 bar at 37 °C was used to support the microemulsion in ethane. Because a pure SCF ethane solvent can only support a W of 5,[15] isooctane was added as a cosolvent [14% (v/v)] to increase surfactant solubility and enhance micelle stability. Complete surfactant solubility was determined through visual observations of the phase behavior using the optical windows in the reactor. The reagent concentrations in this SCF ethane/isooctane mixture were 5 $\times 10^{-2}$ M NaAOT and 5 $\times 10^{-3}$ M $Cu(AOT)_2$ at a W of 7.8. Figure 6 presents the characteristic absorption spectrum of copper nanoparticles produced in the SCF ethane microemulsion system after a reaction time of 1 h. The $\epsilon_{566}/\epsilon_{500}$ ratio from this curve corresponds to particles with a diameter of approximately 9 nm.[7]

Solvent Effects. Several researchers have shown that the bulk solvent type has a strong effect on the micellar exchange rate.[11,24] Figure 7 shows a comparison between the growth rate of copper particles with a W of 5 in liquid isooctane and cyclohexane. In normal liquid solvents, the micellar dynamics is strongly affected by changing the chain length of the oil phase. For example, the micellar exchange rate constants for AOT reverse micelles in cyclohexane, *n*-heptane, and *n*-decane are on the order of 10^6, 10^7, and 10^8 M^{-1} s^{-1}, respectively.[12] The longer chain length liquid solvents have more difficulty penetrating and aligning themselves parallel to the surfactant tails. Consequently, interactions between the AOT tails and the solvent decrease with an increase in the alkyl solvent chain length in these normal liquids.

The effect of supercritical solvent continuous phase properties on the particle growth process can be seen through a comparison of copper particle growth rates in SCF ethane and in normal liquid isooctane at the same temperature and surfactant concentrations. Figure 8 presents a comparison of time-resolved values of the $\epsilon_{566}/\epsilon_{500}$ ratio obtained from spectral measurements of copper nanoparticles for the reaction in normal liquid isooctane at a W of 8 and in SCF ethane with a 14% (v/v) isooctane cosolvent at a W of 7.8. The ratio of $\epsilon_{566}/\epsilon_{500}$ (which correlates with the particle size) in an isooctane solvent demonstrates that the copper particles grow over a period of 3 h, at which time the size asymptotically approaches its limiting value. According to the calibration curve presented by Lisiecki and

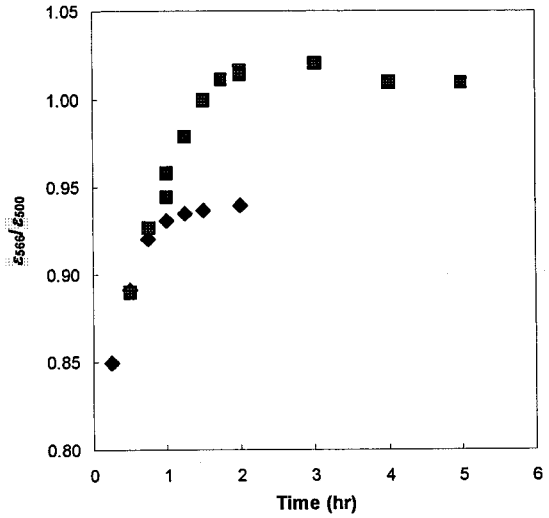

Figure 8. Comparison of $\epsilon_{566}/\epsilon_{500}$ for copper nanoparticles in liquid isooctane (■) at a W value of 7 (T = 37 °C) and SCF ethane/isooctane (◆) at a W of 7.8 based on time-resolved absorption spectra. The surfactant concentrations of the liquid isooctane solutions were [NaAOT] = 5×10^{-1} M and [Cu(AOT)$_2$] = 8×10^{-2} M. The conditions of the ethane experiment were [NaAOT] = 5×10^{-2} M, [Cu(AOT)$_2$] = 5×10^{-3} M, W = 7.8, 14% (v/v) isooctane, P = 245 bar, and T = 37 °C.

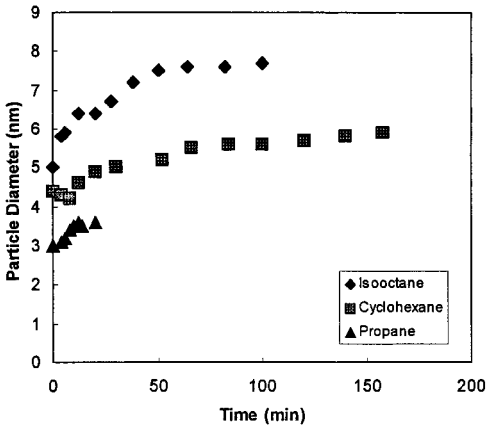

Figure 9. Comparison of the growth of silver particles in various solvents. W_o = 10, T = 25 °C, P = 200 bar (propane), P = 1 bar (isooctane and cyclohexane), [AOT] = 1×10^{-1} M, [$AgNO_3$] = 1×10^{-3} M, and [$NaBH_4$] = 3×10^{-3} M. Particle sizes were calculated from absorption spectra using eq 1 from ref 9.

Pileni,[7] this final ratio corresponds to a particle size of approximately 13 nm. In contrast, the particle growth in SCF ethane may proceed at a slightly faster rate than that in the liquid solvent and is approaching its limiting value after only 2 h. This final ratio of 0.94 in a SCF ethane solution corresponds to a final particle size of 9 nm.[7] This smaller ultimate particle size in ethane may be a result of the lower density and solvent strength of the SCF solvent.

The particle growth rate for silver in compressed propane at 25 °C was also compared to the growth rate in the normal liquid solvents, isooctane and cyclohexane. This comparison is shown in Figure 9. The final particle size is reached in the compressed propane in only 20 min, as opposed to the 50−60 min required in the normal liquid solvents. If eq 1[9] is applied here, the ultimate particle size of 3.7 nm in the lower density propane is significantly smaller than that in the normal liquid solvents. In addition, the appearance of the characteristic peak after only 15 min for the copper particles in propane, as opposed to the hours required in liquids, may be an indication that particle formation occurs more quickly in compressed fluids than in normal liquid solvents.

On the basis of the results in liquid solvents described above, one would expect the ethane to penetrate the surfactant tails effectively, reducing the growth rate. However, the ethane molecules do not interact strongly with and effectively solvate the surfactant.[25] This weak interaction between the ethane solvent and the surfactant tails can result in higher collision frequencies and intermicellar exchange rates. In addition, SCF ethane exhibits higher diffusivity and lower viscosity, density, and dielectric constant than the normal liquid solvents, which can also directly contribute to the enhanced collision frequency and exchange rates between micelles. Therefore, the changed particle growth rates in SCF ethane compared to the normal liquid solvent at the same conditions may be explained by the weak solvating power of the compressed ethane solvent and the intermediate properties (between gas and liquid) of the SCF solvent, resulting in an enhanced intermicellar exchange. Moreover, the slightly smaller final particle size in ethane may be due in part to the inability of a reverse micelle in this lower density medium to support a larger particle.

Conclusions

Reverse micelles in compressed propane and supercritical ethane solvents provide an effective medium for the synthesis of metallic nanoparticles. Nanometer-sized silver particles were produced by the reduction of $AgNO_3$ with $NaBH_4$ in AOT reverse micelles in compressed propane. Also, nanometer-sized copper particles were synthesized by the reduction of copper ions from copper bis(2-ethylhexyl)sulfosuccinate [Cu(AOT)$_2$] incorporated within AOT reverse micelles dispersed in compressed propane and supercritical ethane solutions. Copper particle growth in SCF ethane proceeds at a faster rate than that in the liquid isooctane because of an enhanced intermicellar exchange rate as a result of intermediate physical properties of the SCF solvent and the relatively weak solvating power of the compressed ethane solvent for the AOT reverse micelles. Silver particle growth was found to be faster in the compressed fluid propane compared to that in the normal liquid solvents isooctane and cyclohexane. This work indicates that SCFs may offer a novel way to influence particle synthesis within reverse micelles while providing unique particle recovery methods from solution.

Acknowledgment

This work is based in part upon work supported by the National Science Foundation EPSCoR Program (Grant OSR-9550480) and the Alabama EPSCoR Young Faculty Career Enhancement Program (YFCEP). Their support is gratefully acknowledged. The authors gratefully acknowledge Dr. Michael Miller of the Auburn University Biological Electron Microscopy Imaging Facility for his invaluable assistance with the TEM analysis. We also thank Dr. Jason B. Thompson and Shawn MacInnis for their helpful suggestions and technical support.

Literature Cited

(1) Nalwa, H. S., Ed. *Handbook of Nanostructured Materials & Nanotechnology*; Academic Press: San Diego, 2000.

(2) Adair, J. H.; Li, T.; Kido, K.; Havey, K.; Moon, J.; Mecholsky, J.; Morrone, A.; Tlaham, D. R.; Ludwig, M. H.; Wang, L. *Mater. Sci. Eng.* **1998**, *R23*, 139.
(3) Pileni, M. P.; Lisiecki, I.; Motte, L.; Petit, C.; Cizeron, J.; Moumen, N.; Lixon, P. *Prog. Colloid Polym Sci.* **1993**, *93*, 1.
(4) Pileni, M. P. *J. Phys. Chem.* **1993**, *97*, 6961.
(5) Lisiecki, I.; Lixon, P.; Pileni, M. P. *Prog. Colloid Polym. Sci.* **1991**, *84*, 342.
(6) Pileni, M. P.; Lisiecki, I. *Colloids Surf.* **1993**, *80*, 63.
(7) Lisiecki, I.; Pileni, M. P. *J. Phys. Chem.* **1995**, *99*, 5077.
(8) Barnickel, P.; Wokaun, A.; Sager, W.; Eicke, H.-F. *J. Colloid Interface Sci.* **1992**, *148*, 80.
(9) Petit, C.; Lixon, P.; Pileni, M. P. *J. Phys. Chem.* **1993**, *97*, 12974.
(10) Harai, T.; Sato, H.; Komasawa, I. *Ind. Eng. Chem. Res.* **1994**, *33*, 3262.
(11) Bagwe, R. P.; Khilar, K. C. *Langmuir* **1997**, *13*, 6432.
(12) Fletcher, P. D. I.; Howe, A. M.; Robinson, B. H. *J. Chem. Soc., Faraday Trans. 1* **1987**, *83*, 985.
(13) Natarajan, U.; Handique, K.; Mehra, A.; Bellare, J. R.; Khilar, K. C. *Langmuir* **1996**, *12*, 2670.
(14) McHugh, M. A.; Krukonis, V. J. *Supercritical Fluid Extraction, Principles and Practice*, 2nd ed.; Butterworth-Heinemann: Boston, 1994.
(15) Gale, R. W.; Fulton, J. L.; Smith, R. D. *J. Am. Chem. Soc.* **1987**, *109*, 920−921.
(16) Bartscherer, K. A.; Minier, M.; Renon, H. *Fluid Phase Equilib.* **1995**, *107*, 93.
(17) Matson, D. W.; Fulton, J. L.; Smith, R. D. *Mater. Lett.* **1987**, *6*, 31.
(18) Clarke, M. J.; Harrison, K. L.; Johnston, K. P.; Howdle, S. M. *J. Am. Chem. Soc.* **1997**, *119*, 6399.
(19) Ji, M.; Chen, X.; Wai, C. M.; Fulton, J. L. *J. Am. Chem. Soc.* **1999**, *121*, 2631−2632.
(20) Holmes, J. D.; Bhargava, P. A.; Korgel, B. A.; Johnston, K. P. *Langmuir* **1999**, in press.
(21) (a) Charlé, K. P.; Schulze, W. *Ber. Bunsen-Ges. Phys. Chem.* **1984**, *88*, 350. (b) Kawabata, A.; Kubo, R. *J. Phys. Soc. Jpn.* **1966**, *21*, 1765. (c) Andrews, M. P.; Ozin, G. A. *J. Phys. Chem.* **1986**, *90*, 2929.
(22) Creighton, J. A.; Eadon, D. G. *J. Chem. Soc., Faraday Trans.* **1991**, *87*, 3881.
(23) Yanase, A.; Komiyama, H. *Surf. Sci.* **1991**, *248*, 11.
(24) Towey, T. F.; Khan-Lodhi, A.; Robinson, B. H. *J. Chem. Soc., Faraday Trans.* **1990**, *86*, 3757.
(25) McFann, G. J.; Johnston, K. P. *Langmuir* **1993**, *9*, 2942.

Received for review February 2, 2000
Revised manuscript received September 12, 2000
Accepted September 13, 2000

IE000147Z